Current Biology 23, 453–461, March 18, 2013 ©2013 Elsevier Ltd All rights reserved http://dx.doi.org/10.1016/j.cub.2013.02.033

Article

Recruitment of UBPY and ESCRT Exchange Drive HD-PTP-Dependent Sorting of EGFR to the MVB

Nazim Ali,[1,3] Ling Zhang,[1,3] Sandra Taylor,[1] Alex Mironov,[1] Sylvie Urbé,[2] and Philip Woodman[1,*]
[1]Faculty of Life Sciences, University of Manchester, Manchester M13 9PT, UK
[2]Institute of Translational Medicine, University of Liverpool, Liverpool L69 3BX, UK

Summary

Background: Sorting ubiquitinated epidermal growth factor receptor (EGFR) to the intralumenal vesicles of the multivesicular body requires the coordinated action of several ESCRT complexes. A central question is how EGFR transits vectorially from early, ubiquitin-binding ESCRTs to the final complex, ESCRT-III, such that cargo sequestration is coupled with intralumenal vesicle formation.
Results: We show that the ESCRT accessory protein HD-PTP/PTPN23 associates with EGFR and combines with the deubiquitinating enzyme UBPY/USP8 to transfer EGFR from ESCRT-0 to ESCRT-III and drive EGFR sorting to intralumenal vesicles. HD-PTP binds ESCRT-0 via two interactions with the STAM2 subunit. First, the HD-PTP Bro1 domain binds the core domain of STAM2. This is competed by the ESCRT-III subunit CHMP4B, which binds an overlapping site on HD-PTP Bro1. Second, a proline-rich peptide in HD-PTP binds the SH3 domain of STAM2. Similar proline-rich peptides on UBPY also bind STAM2 SH3 to facilitate EGFR deubiquitination. Hence, locally recruited UBPY would be expected to compete with HD-PTP for STAM2 binding at this second site. Indeed, we show that HD-PTP recruits UBPY to EGFR. Association of UBPY with HD-PTP involves UBPY interacting with HD-PTP-bound CHMP4B, as well as additional interaction(s) between UBPY and HD-PTP.
Conclusions: This study identifies HD-PTP as a central coordinator of the ESCRT pathway for EGFR. Based on these studies, we propose a model whereby the concerted recruitment of CHMP4B and UBPY to HD-PTP and the engagement of UBPY by STAM2 displaces ESCRT-0 from HD-PTP, deubiquitinates EGFR, and releases ESCRT-0 from cargo in favor of ESCRT-III.

Introduction

Activation of EGFR (ErbB1) is followed by its clathrin-dependent endocytosis [1]. Although some EGFR is recycled, a significant portion is ubiquitinated and sorted to intralumenal vesicles (ILVs) within the multivesicular body (MVB) [2], then trafficked to the lysosome. MVB sorting is mediated by the endosomal sorting complex required for sorting (ESCRT) pathway, several protein complexes (ESCRTs 0–III) that collectively drive MVB cargo selection and ILV formation [3–5].

ESCRTs 0–II contain ubiquitin-binding proteins, each of which may help sequester ubiquitinated EGFR. For example, ESCRT-0 is a heterodimer of hepatocyte growth factor regulated substrate (Hrs) and signal transducing adapter molecule (STAM1/2) [6]. Hrs binds ubiquitin via a double-sided ubiquitin interacting motif (DUIM) and a Vps27, Hrs, STAM (VHS) domain [7, 8], whereas STAM contains UIM and VHS domains [8, 9]. ESCRT-I [3] contains the ubiquitin E2 variant (UEV) domain of tumor susceptibility gene 101 (TSG101) [10] and overlapping ubiquitin associated (UBA) domains within ubiquitin associated protein 1 (UBAP1) [11, 12]. Finally, ESCRT-II possesses a GRAM-like ubiquitin-binding motif in EAP45 (GLUE) domain [13].

ESCRT-III appears not to bind ubiquitin directly. This complex, best defined in yeast, assembles on endosomes from cytosolic subunits. First, ESCRT-II recruits and activates one subunit, Vps20p (mammalian charged multivesicular body protein 6 [CHMP6]) [14]. Vps20p seeds assembly of an Snf7p (CHMP4) polymer, which is capped by Vps24p (CHMP3) and Vps2p (CHMP2) [15]. The ESCRT-III polymer is pivotal for membrane deformation and cargo capture into ILVs [4, 15].

Several deubiquitinating enzymes (DUBs) regulate MVB sorting [16]. In particular, two DUBs, associated molecule with the SH3 domain of STAM (AMSH) and ubiquitin specific peptidase 8 (USP8/UBPY), bind to the SH3 domain of STAM and also interact via their microtubule interacting and transport (MIT) domains with multiple ESCRT-III subunits [17–22]. The significance of these DUBs binding both early and late ESCRTs remains unexplained. Indeed, the roles of AMSH and UBPY are controversial. Several studies identify UBPY as promoting EGFR degradation [23–27], but others argue that it "proofreads" ubiquitinated EGFR, allowing the receptor to escape the ESCRT pathway and be recycled [28, 29]. Likewise, "degradative" and proofreading functions have both been ascribed to AMSH [25, 30, 31]. Here we demonstrate that UBPY collaborates with His domain protein tyrosine phosphatase/protein tyrosine phosphatase type N23 (HD-PTP/PTPN23), a regulator of ESCRT-dependent EGFR trafficking [32], to drive EGFR sorting to the MVB.

Results

HD-PTP Is Dispensable for ILV Formation but Essential for Efficient EGFR Sorting

HD-PTP is important for the endosomal transit of EGFR [32]. To detail where HD-PTP acts, we examined EGFR trafficking by EM. Gold-labeled anti-EGFR was bound to cells, which were then pulsed with EGF for ~30 min and subjected to high-pressure freezing to preserve morphology. In control cells, early endosomes (EE) and maturing MVBs contained ILVs labeled with anti-EGFR-gold (Figures 1A and 1B; Table 1). Tomograms revealed associated vesicles, buds and tubules, inward buds, and ILVs (Figure S1A and Movie S1 available online). In contrast, HD-PTP-depleted cells had few isolated EEs/MVBs, and anti-EGFR-gold mainly localized to peripheral tubulovesicular elements and to membrane clusters with complex morphologies and some electron-dense content (Figures 1C and 1D; Table 1). Here, intermembrane filaments were observed, as seen upon TSG101 depletion [33]. However, no obvious build-up of clathrin was seen.

[3]These authors contributed equally to this work
*Correspondence: philip.woodman@manchester.ac.uk

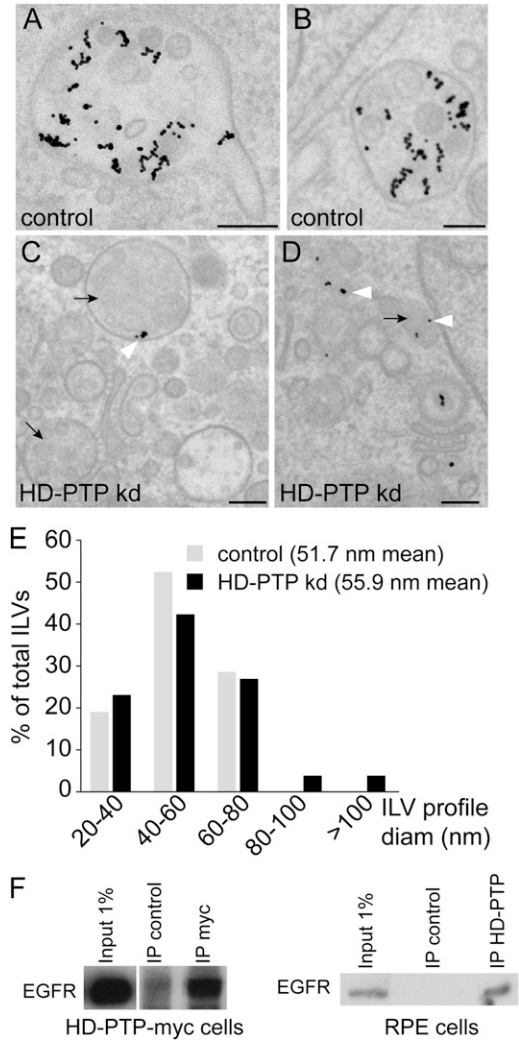

Figure 1. HD-PTP Is Required for EGFR Sorting but Not ILV Formation

(A and B) An early (A) and maturing (B) MVB from control cells after 30 min anti-EGFR-gold uptake.

(C) Anti-EGFR-gold compartments from HD-PTP-depleted HeLa cells. Anti-EGFR-gold, white arrowheads; internal membranes, black arrows.

(D) Another region from HD-PTP-depleted HeLa cells, showing anti-EGFR-gold in tubulovesicular region.

Scale bars represent 200 nm.

(E) Size distribution of ILVs.

(F) IPs, as indicated, were probed by western blot for EGFR.

Table 1. HD-PTP Depletion Disrupts EGFR Trafficking

Compartment	Control (%)	HD-PTP kd (%)
isolated vesicle/tubule (<80 nm diam.)	4.0	15.1
isolated EE/immature MVB	48.4	5.4
isolated LE/mature MVB	47.6	0.9
cluster; vesicle/tubule	–	10.4
cluster; vacuole	–	68.2
all compartments > 80 nm diam.: % α-EGFR lumenal	59.3	10.0

Cells incubated with anti-EGFR-gold were stimulated with EGF for 30 min, then high-pressure frozen for thin-section EM. Gold was scored over each compartment. EE, vacuolar, electron-transluscent endosome with ILVs; LE, electron-dense vacuole with ILVs. Total gold particles in control cells, 798; HD-PTP-depleted cells, 444.

The clusters contained vacuoles resembling MVBs (Figure 1C; Movie S2), though the total cellular MVB content, including those in clusters, was reduced (0.10% ± 0.09% SD relative cell volume density, compared to 0.30% ± 0.11% SD in controls). 68.2% of anti-EGFR-gold had reached vacuoles, but 92% of this remained at the limiting membranes (Figure 1C; Table 1). By comparison, only 40% of EGFR in MVBs of control cells was at the limiting membranes. Despite this defect, ILVs were abundant (Figure 1C, arrows; Figure S1C; Movie S2), accounting for 18.4% ± 9.6% of MVB volume versus 19.7% ± 6.7% in controls. Some yeast ESCRT mutants allow ILVs to form, albeit abnormally sized [34]. ILVs in HD-PTP-depleted cells were similarly sized to those in control cells, except for a few larger structures (Figure 1E). Clusters also included tubulovesicular regions (Figure 1D), with interconnected and sometimes sheet-like elements (Figure S1D; Movie S3). Though intralumenal membranes were present (Figure 1D, arrows), all anti-EGFR-gold within these regions remained at the limiting membranes (Figure 1D). Less anti-EGFR-gold was internalized in HD-PTP-depleted cells, implying fewer cell surface EGFR. Indeed, although total EGFR was reduced only slightly, significant quantities of EGFR mislocalized to internal membranes in unstimulated cells, consistent with reported defects in constitutive recycling as well as degradative pathways [32] (Figures S1E and S1F).

In conclusion, HD-PTP loss affects endosome morphology and disrupts two aspects of EGFR trafficking. More EGFR is retained in tubules/vesicles, consistent with reduced transit to larger endosomes and implying that HD-PTP may play an as yet undetermined role in membrane fusion. Principally, however, EGFR sorting to the lumen of vacuoles is inhibited, despite normal ILVs continuing to form. By contrast, loss of ESCRT-I abrogates both cargo sorting and normal ILV generation [33, 35]. Consistent with HD-PTP engaging EGFR with the MVB pathway, EGFR coimmunoprecipitated with epitope-tagged or endogenous HD-PTP (Figure 1F).

HD-PTP Binds STAM2 at Two Sites

HD-PTP binds the ESCRT-III subunit CHMP4B within its Bro1 domain [32, 36] and the ESCRT-I component UBAP1 within its putative V domain [11] (see Figure 2A). To further investigate how HDPTP integrates with the ESCRT pathway, we screened the Bro1-V fragment, which provides the minimal essential unit supporting the endocytic function of HD-PTP [32], by yeast two-hybrid (Y2H) against a cDNA library. This identified five clones containing aa 267–416 of STAM2 (see Figure 2A). Based on structural studies of the STAM1/Hrs dimer [6], this region spans the STAM2 "core" domain, which binds Hrs. Directed Y2H via full-length STAM2 confirmed the interaction, with full-length HD-PTP binding somewhat more strongly (Figures S2A and S2B). STAM2 did not bind to the Bro1-V fragment of Alix, a protein related to HD-PTP that acts during viral budding and cytokinesis [37] (Figures S2A and S2B). Alix Bro1-V was folded, since it bound CHMP4B (Figure S2A), as reported [36, 38].

STAM2 bound the HD-PTP Bro1 domain, but not the V domain (Figures S2A and S2C). Binding was compromised by a mutation (L202D/I206D; L/I-D/D) that disrupts HD-PTP Bro1 binding to CHMP4B [32] (Figures S2A and S2D). This mutant appears folded, since it binds UBAP1 (Figure S2E). Bacterially expressed His_6-HD-PTP Bro1-V bound in vitro

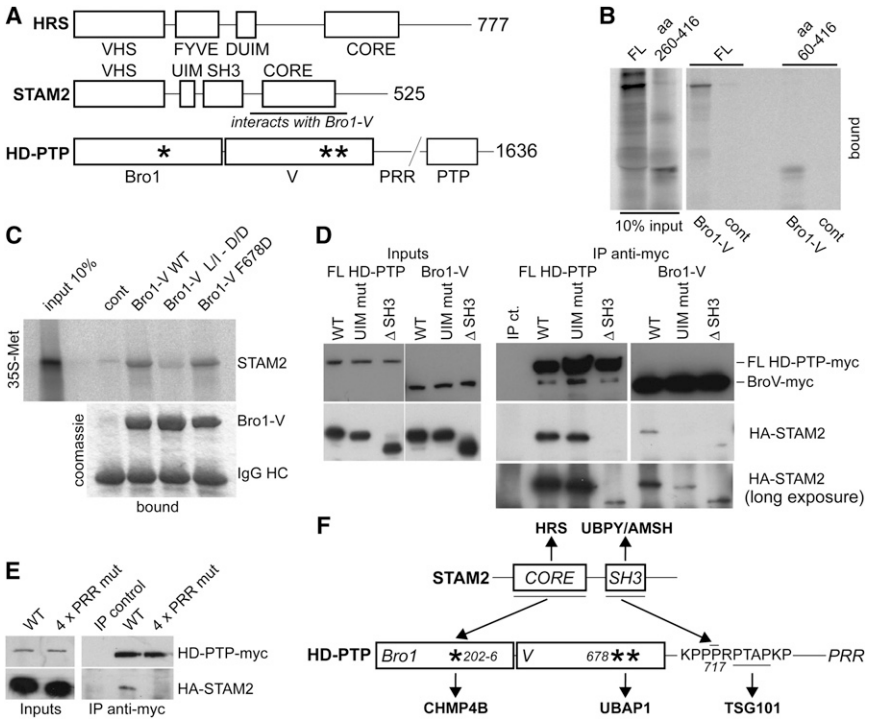

Figure 2. HD-PTP Binds to STAM2 at Two Sites

(A) Organization of HD-PTP, STAM2, and Hrs. Single asterisk indicates CHMP4 binding site; double asterisk indicates UBAP1 binding site.

(B) Translated STAM2 or STAM2(260-416) were assayed for binding to His_6-HD-PTP Bro1-V WT.

(C) Translated STAM2 binding to His_6-HD-PTP Bro1-V WT or mutants (bottom panel shows Coomassie stain of the anti-His_6 IP).

(D) IPs from HD-PTP-myc or HD-PTP Bro1-V-myc cells, transfected with HA-STAM2 constructs, were analyzed by WB.

(E) IPs from HelaM cells cotransfected with HA-STAM2 plus WT HD-PTP-myc, or HD-PTP-myc with SH3 binding mutations (4 × PRR mut), were analyzed by WB.

(F) Diagram summarizing how STAM2 binds HD-PTP and other effectors (aa residues in italics).

translated STAM2 or the STAM2 core domain (Figure 2B). Binding was likewise compromised by the L/I-D/D mutation but not by a mutation (F678D) that prevents HD-PTP binding to UBAP1 [11] (Figure 2C). Hence, ESCRT-0 and ESCRT-III may occupy overlapping sites within the HD-PTP Bro1 domain.

Immunoprecipitations from cells expressing HD-PTP-myc and HA-STAM2 constructs pointed to additional modes of binding (Figures 2D and S2F). Specifically, full-length HD-PTP-myc bound STAM2 much more efficiently than did HD-PTP Bro1-V (Figure 2D), extending our initial observations by Y2H (Figure S2B). A mutation (L176A/S177A) that abolishes STAM2 UIM activity [30] reduced STAM2 binding to HD-PTP Bro1-V-myc (Figure 2D). Hence, this interaction may be regulated by ubiquitin binding, though we have not explored this further. In contrast, deletion of the STAM2 SH3 domain dramatically reduced interaction between STAM2 and full-length HD-PTP (Figure 2D).

We therefore searched for potential STAM2 SH3-binding peptides in HD-PTP. Two peptides (KKPPPRP and PLLPRR) localized to a stretch (K^{714}KPPPRPTAPKPLLPRR^{730}) immediately distal to the V domain and including a PTAP motif that binds TSG101 [36]. This also contains the sequence PPPRPTAPKP, which binds the Mona SH3 domain [39] and closely resembles the PXXXRXXKP motifs in UBPY [21, 28] and AMSH [20] that bind STAM SH3. A mutation (P716A,P717A,P728A,R730A) in HD-PTP-myc reduced HA-STAM2 binding substantially (Figure 2E). To fine-map the interaction, we employed Y2H as a more sensitive assay. Here, binding between full-length STAM2 and HD-PTP was not affected by the L/I-D/D (CHMP4B binding) mutation or by additional mutation of P716 but was lost when P717 was mutated (Figure S2G). Mutants lacking P717 still bound TSG101, and hence were expressed normally (Figure S2G). As expected, a P716A,P717A mutant bound STAM2 if the Bro1 domain was wild-type. In summary, STAM2 binds to HD-PTP via two sites that contribute to other molecular interactions (Figure 2F).

In cells, STAM2 and Hrs form ESCRT-0. HD-PTP associated with endogenous ESCRT-0, as evidenced by its coimmunoprecipitation with Hrs and STAM2 (Figures 3A–3C) and the precise colocalization of Hrs and HD-PTP (Figure 3D; color merge in Figure S3). Binding of HD-PTP to both EGFR and ESCRT-0 occurred in serum-starved cells but increased slightly within 2.5 min of EGFR activation. Clearly, however, these interactions declined after 15–30 min (Figure 3E). Because ESCRT-0 interacts with EGFR [40, 41], it was possible that association of HD-PTP with EGFR occurred via ESCRT-0. However, depleting Hrs by siRNA (which also depletes STAM [42]) did not alter HD-PTP binding to EGFR (Figure 3F). In summary, HD-PTP associates with ESCRT-0 and is released after EGFR activation.

HD-PTP Controls Transfer of EGFR from ESCRT-0 to ESCRT-III

HD-PTP interacts with cargo and multiple ESCRTs and is required to translocate EGFR into ILVs. Hence, HD-PTP may help to transfer EGFR from ESCRT-0, which sequesters ubiquitinated cargoes, through to ESCRT-III, which drives ILV formation. If this were the case, we would expect that HD-PTP depletion would impair the release of ESCRT-0 from EGFR and prevent EGFR from associating with ESCRT-III.

We first assessed the timing of EGFR association with ESCRT-0 in control cells. As shown previously [41], we detected a wave of EGFR associating with Hrs 2–5 min after EGF stimulation, before declining over 15–30 min (Figure 4A). We also examined endogenous EGFR-Hrs association in intact cells, using the Duolink proximity ligation assay (PLA) [43]. Here also, levels of Hrs-EGFR association rose sharply soon after EGF stimulation, before declining (Figure 4B).

We next examined how depleting HD-PTP affected EGFR-ESCRT interactions, focusing initially on ESCRT-0. Levels of both Hrs and STAM2 were reduced in HD-PTP-depleted cells (Figures 4C and S4A). This could not account for the impairment in EGFR sorting, however, because ESCRT-0 depletion generates a quite distinct EGFR-sorting defect ([35]; our unpublished data). In addition, treatment of HD-PTP-depleted cells for 8 hr with the reversible EGFR inhibitor Iressa partially restored ESCRT-0 levels (Figure S4B) but did not restore the

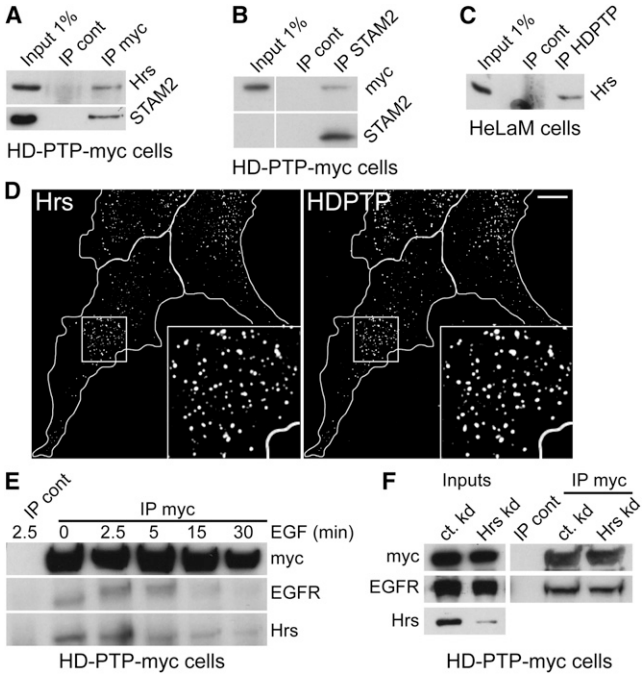

Figure 3. HD-PTP Associates with ESCRT-0

(A and B) Lysates from HD-PTP-myc-expressing cells were immunoprecipitated with anti-myc (A) and anti-STAM2 (B) and probed by WB.

(C) An HD-PTP immunoprecipitate from cell lysates was probed with anti-Hrs.

(D) RPE cells were immunostained for endogenous Hrs and HD-PTP. Scale bar represents 10 μm.

(E) Lysates from cells challenged with EGF as indicated were immunoprecipitated and probed by WB. A control IP was from cells stimulated with EGF for 2.5 min.

(F) Lysates from control or Hrs-depleted cells were immunoprecipitated and probed by WB.

EGF transport defect in subsequent experiments (Figure S4C). Intriguingly, ESCRT-0 turnover is dependent on Cbl ubiquitin ligase and may be linked to its phosphorylation cycle [44]. Hence, the pronounced loss of ESCRT-0 we observed may point to an impaired functional cycle caused by loss of HD-PTP. Indeed, consistent with reduced ESCRT-0 release from endosomes, virtually all the remaining ESCRT-0 was membrane associated, in contrast to its mainly cytosolic distribution in control cells (Figure S4D).

Strikingly, despite diminished Hrs, more Hrs was found in EGFR immunoprecipitates from unstimulated HD-PTP-depleted cells compared to controls (Figure 4D), consistent with a failure to release ESCRT-0 fully from cargo. Indeed, the proximity ligation assay showed that in contrast to the dynamic association of ESCRT-0 and EGFR seen after stimulating control cells with EGF, this association was stable and EGF independent upon HD-PTP depletion (Figure 4E). Hence, HD-PTP helps release EGFR from ESCRT-0. These effects on ESCRT-0 were not simply due to general disruption of ESCRT function, because depletion of the ESCRT-I subunit TSG101 did not alter Hrs levels (Figure S4E). Although Hrs-EGFR association increased somewhat in TSG101-depleted cells, this increase was clearly weaker than the effect of HD-PTP depletion (Figure S4E).

To assess the interaction of EGFR with ESCRT-III, we expressed myc-tagged CHMP4B. EGFR coimmunoprecipitated with CHMP4B-myc in extracts from control cells challenged with EGF for 15 min but not from HD-PTP-depleted cells (Figure 4F). In conclusion, the changes in EGFR-ESCRT binding and failure in EGFR sorting observed upon HD-PTP depletion suggest that HD-PTP may act to release EGFR from ESCRT-0 and subsequently allow it to engage ESCRT-III.

HD-PTP Combines ESCRT Competition with UBPY Recruitment to Sort EGFR

The overlapping STAM2 and CHMP4B binding sites within the Bro1 domain might contribute to the ability of HD-PTP to switch EGFR from ESCRT-0 to ESCRT-III. We therefore tested whether STAM2 and CHMP4B do indeed compete for HD-PTP binding at this site. GST-CHMP4B, but not GST, bound efficiently to His_6-HD-PTP Bro1-V and interfered with the binding of in vitro translated STAM2 (Figure 5A). To examine ESCRT competition in a cellular context, we used the proximity ligation assay to measure association between stably expressed HD-PTP-myc and endogenous CHMP4B, using an antibody that is highly specific for CHMP4B among ESCRT-III subunits (Figure S5A). This signal was not affected in cells expressing GFP alone, but was significantly reduced in cells expressing GFP and cotransfected with HA-STAM2 (Figure S5B; $p < 0.001$).

Although these data are consistent with an exchange occurring between ESCRT-0 and ESCRT-III on HD-PTP, additional mechanism(s) must be in play to release ESCRT-0 from HD-PTP and EGFR and account for the vectorial transit of cargo through the ESCRT pathway. We focused on the interaction of the STAM2 SH3 domain with the proline-rich peptide of HD-PTP, because STAM2 binds three similar peptides within UBPY [21, 28]. Hence, locally recruited UBPY might aid the displacement of STAM2 from HD-PTP. Intriguingly, the phenotypes of UBPY and HD-PTP depletion resemble each other in several respects, including the destabilization of ESCRT-0 [23]. Additionally, *S. cerevisiae* Bro1p recruits and activates Doa4p, the yeast ortholog of UBPY [34, 45]. We therefore asked whether HD-PTP helps recruit UBPY to EGFR. Indeed, depleting HD-PTP prevented endogenous UBPY from associating with EGFR (Figure 5B), consistent with increased EGFR ubiquitination (Figure S5C). The failure to recruit UBPY to EGFR was not due simply to the reduction in ESCRT-0 levels caused by HD-PTP depletion, since siRNA of Hrs, which reduced Hrs levels still further (Figure S5D), did not affect UBPY-EGFR association (Figure S5E).

In keeping with the importance of HD-PTP for recruiting UBPY to EGFR, endogenous UBPY coimmunoprecipitated with HD-PTP-myc from cell lysates (Figure 5C). UBPY also coimmunoprecipitated with the Bro1-V fragment of HD-PTP but less efficiently (Figure 5C). Hence, like STAM2, UBPY may bind HD-PTP at multiple sites. We investigated in more detail how UBPY bound HD-PTP Bro1-V. We focused on the N-terminal MIT domain of UBPY, which also binds CHMP4B, because this is essential for recruiting UBPY to endosomes and supporting EGFR degradation [19]. Moreover, *S. cerevisiae* Bro1p recruits Doa4p to the endosome via an interaction between the N-terminal regions of each protein [34].

Binding of GST-UBPY MIT to His_6-HD-PTP Bro1-V was not detected (Figures 5D and S5F). However, when GST-CHMP4B was also provided, efficient recruitment of GST-UBPY MIT, but not GST, to His_6-HD-PTP Bro1-V was observed. In contrast, binding of CHMP4B to His_6-HD-PTP Bro1-V was not influenced by UBPY MIT. Altogether, these data indicate that CHMP4B binds the MIT domain of UBPY and the HD-PTP

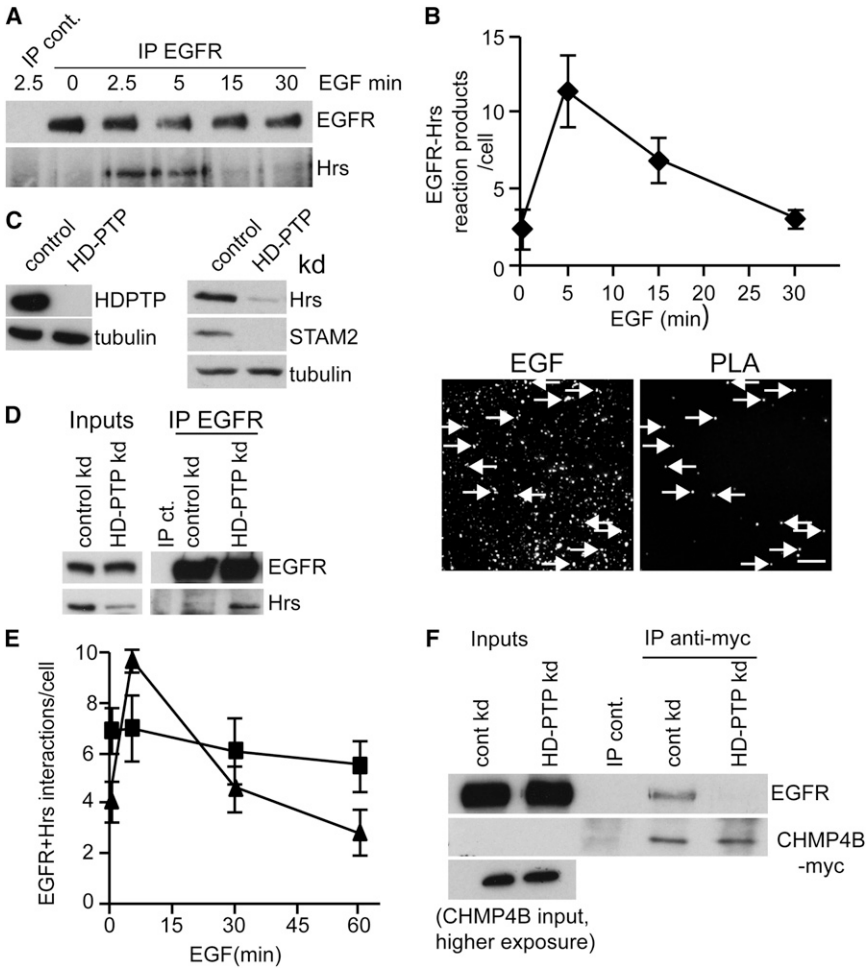

Figure 4. Loss of HD-PTP Affects Transfer of EGFR from ESCRT-0 to ESCRT-III

(A) IPs of lysates from HeLaM cells, challenged with EGF, were probed by WB.

(B) Top: PLA analysis of EGFR-Hrs association in cells pulsed with EGF. Values are means ± SD from three experiments. Bottom: Representative image showing EGFR-Hrs PLA product colocalizing with Alexa 488-EGF after 5 min uptake (arrows).

(C) HeLaM cell extracts were analyzed by WB.

(D) EGFR IPs were analyzed by WB.

(E) PLA of EGFR-Hrs association in control (triangles) or HD-PTP-depleted (squares) cells after EGF stimulation. Values are means ± SD from three experiments.

(F) IPs from cells expressing CHMP4B-myc, 15 min after treatment with EGF, were analyzed by WB.

Bro1 domain simultaneously, though it is formally possible that CHMP4B additionally activates UBPY MIT to bind HD-PTP Bro1-V directly. To test for additional UBPY binding sites within HD-PTP, we examined the ability of full-length HD-PTP L/I-D/D to bind UBPY, because this mutant cannot bind CHMP4B (Figure S2D). Binding was not affected significantly (Figure 5E).

These binding reactions provide a scenario in which UBPY could aid transit of EGFR to ESCRT-III by helping to displace STAM2 from HD-PTP (Figure S5G). Loss of UBPY function enhances EGFR ubiquitination, but studies differ in their conclusions about how this affects EGFR trafficking [19, 23–29]. We therefore examined in detail the consequences of UBPY depletion (Figure S6A). First, fluorescent EGF and EGFR degradation was impaired, and ubiquitinated proteins accumulated on endosomes (Figures S6B and S6C), as described previously with different siRNA oligonucleotides [19, 23] and as also seen upon HD-PTP depletion (Figure S6D).

We then tested by EM whether UBPY is important for MVB sorting of EGFR. UBPY depletion disrupted anti-EGFR-gold trafficking to mature MVBs and lysosomes (Table S1) and induced endosome morphologies reminiscent of, albeit somewhat milder than, those seen with HD-PTP depletion (Figures 6A, 6B, and S6E; Movie S4). Features typifying UBPY depletion included endosomal clusters, as shown previously [23], but generally less extensive than those seen after depleting HD-PTP (Figure 6A, panels i, iii); MVBs with apparently normal morphologies but reduced lumenal anti-EGFR-gold (Figure 6A, panels ii, iii); and swollen endosomes containing large membrane inclusions as well as abundant ILVs, with anti-EGFR-gold located mainly at the limiting membrane (Figure 6A, panel iv; Figure S6E; Movie S4). Quantitative analysis showed a delay in anti-EGFR-gold sorting to the lumen, with only 39.0% entering the lumen of compartments after 30 min, compared to 83.3% in control cells (Figure 6B; Table S1). However, this defect was less severe than that caused by HD-PTP depletion. Most anti-EGFR-gold eventually reached the lumen of late endosomes or lysosomes, though transit to lysosomes was relatively inefficient (Table S1). In keeping with this intermediate phenotype, UBPY depletion partially reduced the interaction of EGFR with ESCRT-III (Figure 6C). In summary, we conclude that HD-PTP plays an obligate role in EGFR transit to ESCRT-III and MVB sorting, while UBPY functions to facilitate this pathway (Figure 6D).

Discussion

In this study we identify an essential role for HD-PTP in sorting EGFR to ILVs within the MVB, but not for ILV formation per se. UBPY also contributes to EGFR sorting. Yeast *Doa4* mutants, or *Bro1* mutants unable to bind Doa4p [34], also result in defective cargo sorting while maintaining ILV formation. Collectively, these data point to a central role for Bro1 proteins and endosomal DUBs in allowing ubiquitinated endocytic cargo to engage productively with the ESCRT pathway. Although we show that HD-PTP associates with EGFR, we as yet do not know whether HD-PTP binds EGFR directly, nor whether it regulates the trafficking of other signaling receptors. Certainly, the presence of normal ILVs in cells lacking HD-PTP implies the existence of other cargo entry routes into the MVB (notwithstanding the possibility that ILVs could form without cargo). The HD-PTP-related protein Alix participates in multiple ESCRT pathways but is dispensable for efficient EGFR sorting [24, 32]. However, recent reports identify substrates for Alix-dependent ILV-sorting pathways [46], in

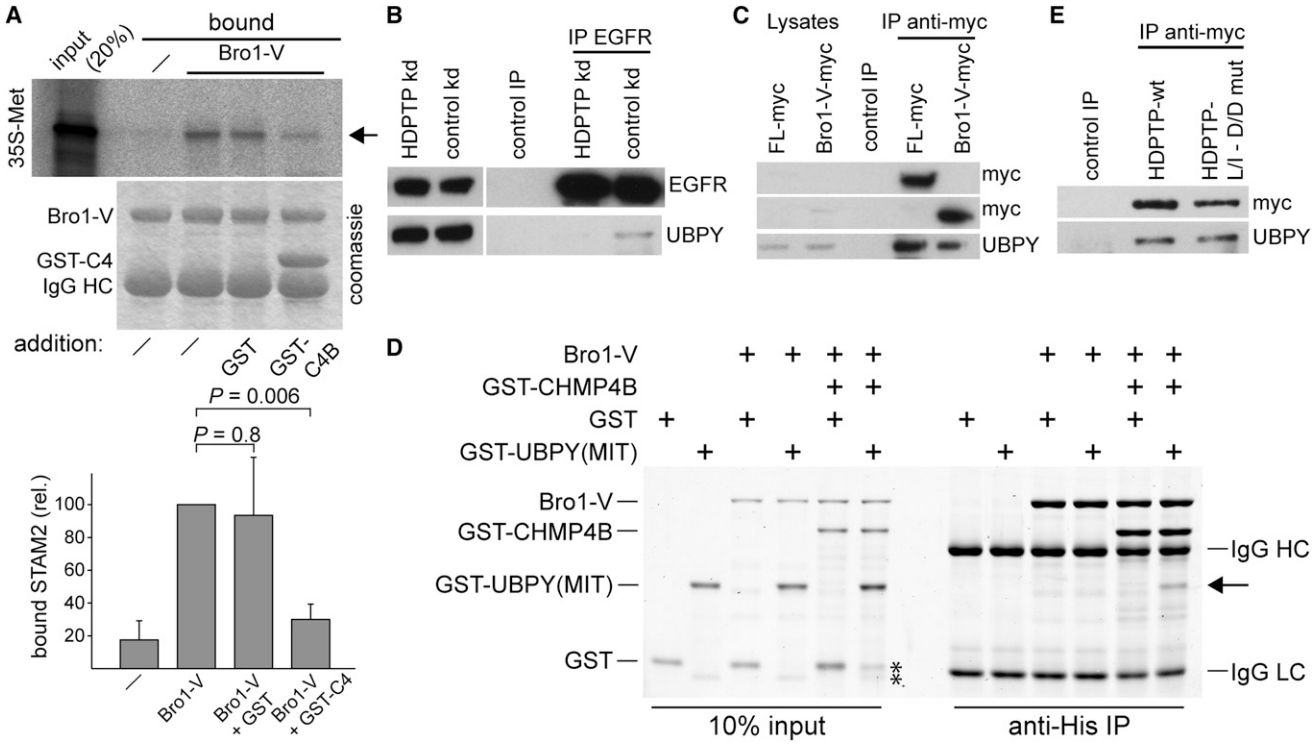

Figure 5. ESCRT-III and UBPY Displace ESCRT-0 from HD-PTP

(A) Left: Translated STAM2 was assayed for binding to His_6-HD-PTP Bro1-V with or without GST-CHMP4B. Bottom: Quantitation from three experiments ± SD.
(B) EGFR IPs were probed by WB.
(C and E) Myc IPs from cells expressing HD-PTP-myc constructs (C) or WT or mutated HD-PTP-myc (E) were probed by WB.
(D) His_6-HD-PTP Bro1-V was incubated with or without GST-CHMP4B and either GST or GST-UBPY MIT. Samples were Coomassie stained (or blotted for GST; Figure S5F); arrow shows GST-UBPY MIT. Asterisks show degradation products.

keeping with previous studies implicating Alix in MVB biogenesis [47].

Our work shows that HD-PTP function is closely linked with ESCRT-0, with two binding modes identified. That involving the Bro1 domain appears selective, since we could not detect binding between STAM2 and Alix Bro1. This matches the functional specificity of each Bro1 protein and extends our previous observation that the HD-PTP V domain selectively binds UBAP1, a component of an ESCRT-I complex important for endosomal sorting of ubiquitinated cargoes but not for cytokinesis [11, 12]. The overall architectures of the HD-PTP and Alix Bro1 domains are similar, including the CHMP4B binding groove [48]. However, the structures differ in several respects, such as the loop centered on Phe105 that confers a selective ability of Alix to bind HIV-1 Gag [48]. The specific binding of STAM2 to HD-PTP suggests that it contacts the Bro1 domain beyond the CHMP4B binding groove, though our data also indicate that STAM2 and CHMP4B binding are incompatible with each other.

As our study highlights, the presence of such overlapping binding sites provides the potential for HD-PTP to switch ESCRTs, supporting its action during EGFR sorting. Critically, however, further mechanisms must ensure that movement of cargo through the ESCRT pathway is vectorial. We provide evidence that UBPY forms one component of this regulatory process. Based on our findings and those in the literature, UBPY may have a dual function. First, the coordinated recruitment of CHMP4B and UBPY to HD-PTP would bring about exchange reactions that disrupt both modes of STAM2 binding to HD-PTP (Figure 6D). Second, deubiquitination of cargo by UBPY would favor association of ESCRT-III over ESCRT-0 with a HD-PTP-cargo complex, given the importance of multivalent ubiquitin binding in allowing ESCRT-0 to sequester cargo [3, 8, 49]. Consistent with this model, both its catalytic activity and the MIT domain are essential for UBPY function during EGFR trafficking [19, 23]. *S. cerevisiae* Bro1p binds ESCRT-I and ESCRT-III [45] and is important for recruiting Doa4p to cargo [34, 45]. Additionally, however, Bro1p activates Doa4p catalytic activity [34], and it is possible that HD-PTP fulfils a similar role to couple ESCRT exchange more completely with cargo deubiquitination. Although UBPY-dependent deubiquitination facilitates vectorial transit of EGFR, it is not obligate for ILV sorting, in keeping with the ability of artificial cargoes fused to ubiquitin to sort to the MVB [49].

Our study provides a rational basis for explaining exchange between early and late ESCRTs. However, further mechanisms must direct and regulate this process. First, ESCRT-I is also essential for EGFR sorting [33]. While HD-PTP interacts with ESCRT-I via two PTAP motifs within its PRR that bind TSG101 [36] and via binding to UBAP1 [11], much more work is needed to ascertain precisely how ESCRT-I function is linked to that of HD-PTP. Additional factors that may provide directionality to an ESCRT exchange reaction include the polymerization of ESCRT-III and subsequent entrapment of EGFR within the developing ILV that would render it incapable of re-engaging ESCRT-0 and the influence of tyrosine phosphorylation and PTPases on the activity status of ESCRTs [50]. In this

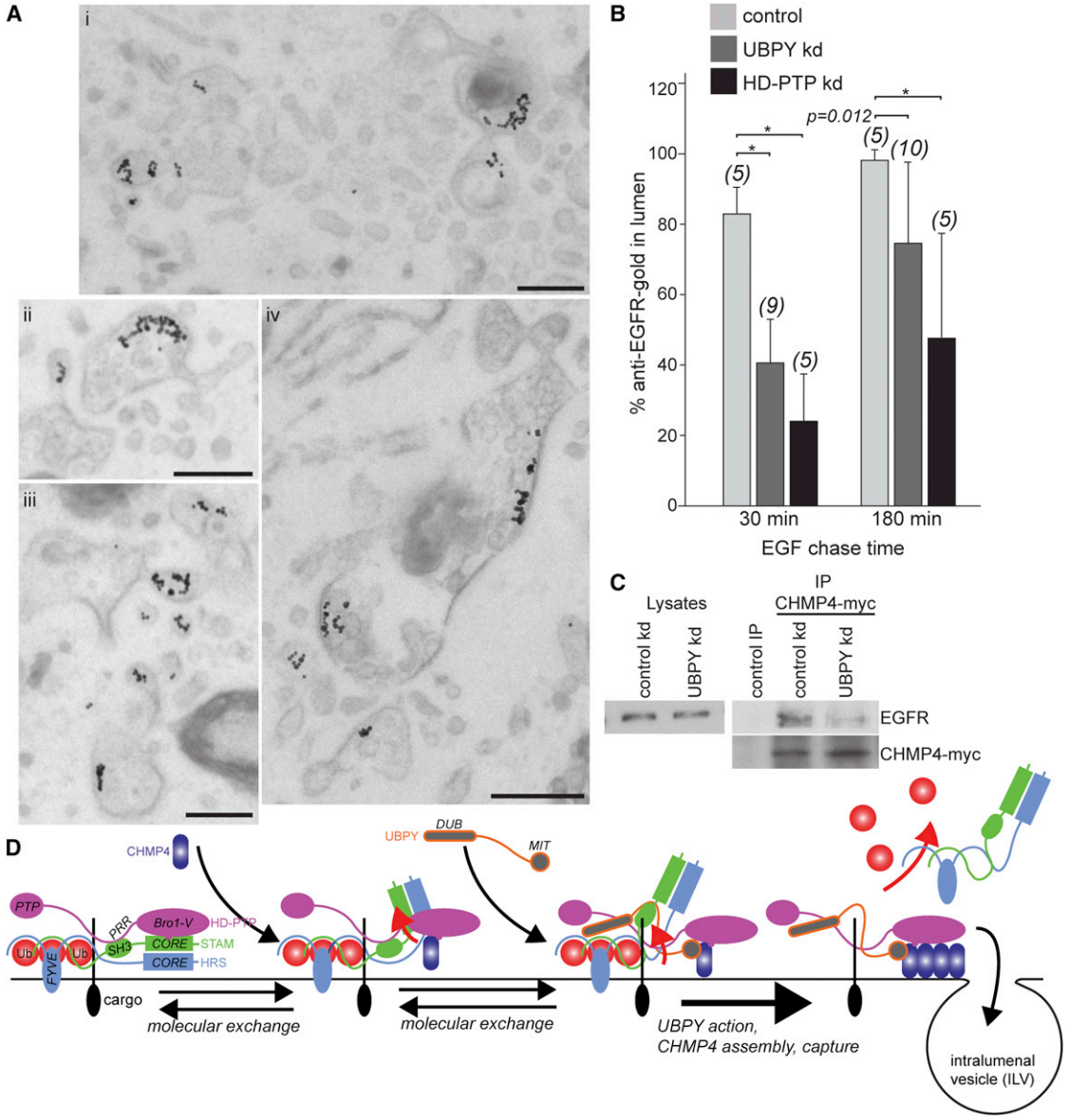

Figure 6. UBPY Facilitates EGFR Sorting to the MVB

(A) Representative endocytic compartments from UBPY-depleted cells after 30 anti-EGFR-gold uptake. Scale bars represent 200 nm.

(B) Percentage of anti-EGFR-gold in lumen of all compartments; see also Table S1. Values are means ± SD from the indicated number of cells (brackets). *p < 0.001.

(C) Anti-myc IPs from cells expressing CHMP4B-myc (15 min treatment with EGF) were analyzed by WB.

(D) A model for HD-PTP and UBPY function. HD-PTP first binds EGFR and ESCRT-0. Recruitment of CHMP4B and UBPY to HD-PTP displaces STAM2/ESCRT-0 from HD-PTP. In conjunction, STAM2 binding facilitates UBPY-dependent deubiquitination of EGFR, supporting release of ESCRT-0 from EGFR in favor of ESCRT-III.

context, the possible PTPase function of HD-PTP may be significant. A further point of investigation is at what point, if at all, HD-PTP is released from ILV-bound EGFR.

Experimental Procedures

Reagents

A list of cell lines, antibodies, molecular biology and transfection reagents is in Supplemental Experimental Procedures.

Yeast Two Hybrid

Y2H screening was performed by Hybrigenics, S.A. (Paris, France) (http://www.hybrigenics-services.com). Directed two-hybrid used Matchmaker Gold (Clontech). Full details are in Supplemental Experimental Procedures.

Immunoprecipitations

For native IPs, cells were lysed in IP buffer (25 mM Tris-HCl [pH 7.5], 40 mM NaCl, 0.5% IGEPAL) containing PIC-III (Sigma). Denaturing IPs used RIPA buffer (IP buffer also containing 0.1% SDS, 1% sodium deoxycholate, 50 mM NaF, 2 mM Na_3VO_4, 10 mM NEM). Lysates were clarified at 14,000 rpm for 15 min at 4°C and incubated with antibodies at 4°C overnight, then 3–4 hr with protein A sepharose (Zymed), preblocked with 50 mg/ml BSA. Beads were washed four times in IP buffer, then analyzed by western blot (WB). Control IPs used nonimmune sera or IgGs. To analyze total extracts only, cells were lysed in IP buffer containing 0.1% SDS and clarified. Western blots used HRP-secondary antibodies and ECL, or Li-Cor

secondary antibodies. Panels for all figures have been cut from the same exposures unless stipulated in the figure legend.

Pull-Down Experiments

Translations of PCR products using [^{35}S]methionine and nuclease-treated reticulocyte lysates (Promega) were terminated with 1 mM puromycin. Products were incubated with 5 μg His_6-HD-PTP Bro1-V in 50 mM HEPES (pH 7.4), 100 mM NaCl, 0.1% Triton X-100 (Anatrace), 1 mM methionine, and PIC-III for 4–6 hr at 4°C. Incubations were clarified with protein A-sepharose. Anti-His_6 (4 μl) was added and IPs continued as above. Samples were analyzed by phosphorimager. A similar protocol was used to examine binding of GST-fusion proteins.

Subcellular Fractionation

Cells (2 × 15 cm dishes per sample) were trypsinized, collected in 50 ml complete medium, and pelleted at 1,500 rpm for 5 min at 4°C. Cells were washed twice with buffer A (3 mM Mg acetate, 5 mM EGTA, 10 mM HEPES [pH 7.4], 250 mM sucrose), resuspended in 2 ml buffer A containing PIC-III and 1 mM DTT, and homogenized with a ball-bearing homogenizer (Isobiotec, Germany). A postnuclear supernatant was prepared by centrifuging twice at 3,000 rpm for 10 min, and 1.5 ml was loaded on a 25% sucrose cushion in buffer A (800 μl) and centrifuged at 200,000 × *g* for 30 min at 4°C. The cytosol was removed and the pellet washed with buffer A and solubilized directly into SDS-PAGE buffer.

Immunofluorescence and Imaging

Pulse-chase experiments with Alexa 488-EGF were performed as described, with EGF pulsed for 3 min at 37°C and chased in unlabelled medium [11]. Details of IF labeling conditions and image acquisition are in Supplemental Experimental Procedures. The Duolink PLA system (OLink Bioscience) was used according to the manufacturer's instructions.

Electron Microscopy

For EM pulse-chase analysis, 18 nm colloidal gold was conjugated to affinity-purified anti-EGFR, MAb 108. Cells were subjected to high-pressure freezing or conventional fixation as indicated. Reagent preparation, sample processing, and quantitation details are in Supplemental Experimental Procedures.

Supplemental Information

Supplemental Information includes Supplemental Experimental Procedures, six figures, one table, and four movies and can be found with this article online at http://dx.doi.org/10.1016/j.cub.2013.02.033.

Acknowledgments

This work is supported by the MRC (G0701141 and G0900930) and BBSRC (BB/I012109/1). We thank Viki Allan, Stephen High, and Martin Lowe for discussions and the FLS EM and bioimaging facilities.

Received: October 31, 2012
Revised: February 4, 2013
Accepted: February 14, 2013
Published: March 7, 2013

References

1. Goh, L.K., Huang, F., Kim, W., Gygi, S., and Sorkin, A. (2010). Multiple mechanisms collectively regulate clathrin-mediated endocytosis of the epidermal growth factor receptor. J. Cell Biol. *189*, 871–883.
2. Eden, E.R., Huang, F., Sorkin, A., and Futter, C.E. (2012). The role of EGF receptor ubiquitination in regulating its intracellular traffic. Traffic *13*, 329–337.
3. Hurley, J.H., and Hanson, P.I. (2010). Membrane budding and scission by the ESCRT machinery: it's all in the neck. Nat. Rev. Mol. Cell Biol. *11*, 556–566.
4. Wollert, T., and Hurley, J.H. (2010). Molecular mechanism of multivesicular body biogenesis by ESCRT complexes. Nature *464*, 864–869.
5. Henne, W.M., Buchkovich, N.J., and Emr, S.D. (2011). The ESCRT pathway. Dev. Cell *21*, 77–91.
6. Ren, X., Kloer, D.P., Kim, Y.C., Ghirlando, R., Saidi, L.F., Hummer, G., and Hurley, J.H. (2009). Hybrid structural model of the complete human ESCRT-0 complex. Structure *17*, 406–416.
7. Hirano, S., Kawasaki, M., Ura, H., Kato, R., Raiborg, C., Stenmark, H., and Wakatsuki, S. (2006). Double-sided ubiquitin binding of Hrs-UIM in endosomal protein sorting. Nat. Struct. Mol. Biol. *13*, 272–277.
8. Ren, X., and Hurley, J.H. (2010). VHS domains of ESCRT-0 cooperate in high-avidity binding to polyubiquitinated cargo. EMBO J. *29*, 1045–1054.
9. Mizuno, E., Kawahata, K., Kato, M., Kitamura, N., and Komada, M. (2003). STAM proteins bind ubiquitinated proteins on the early endosome via the VHS domain and ubiquitin-interacting motif. Mol. Biol. Cell *14*, 3675–3689.
10. Garrus, J.E., von Schwedler, U.K., Pornillos, O.W., Morham, S.G., Zavitz, K.H., Wang, H.E., Wettstein, D.A., Stray, K.M., Côté, M., Rich, R.L., et al. (2001). Tsg101 and the vacuolar protein sorting pathway are essential for HIV-1 budding. Cell *107*, 55–65.
11. Stefani, F., Zhang, L., Taylor, S., Donovan, J., Rollinson, S., Doyotte, A., Brownhill, K., Bennion, J., Pickering-Brown, S., and Woodman, P. (2011). UBAP1 is a component of an endosome-specific ESCRT-I complex that is essential for MVB sorting. Curr. Biol. *21*, 1245–1250.
12. Agromayor, M., Soler, N., Caballe, A., Kueck, T., Freund, S.M., Allen, M.D., Bycroft, M., Perisic, O., Ye, Y., McDonald, B., et al. (2012). The UBAP1 subunit of ESCRT-I interacts with ubiquitin via a SOUBA domain. Structure *20*, 414–428.
13. Slagsvold, T., Aasland, R., Hirano, S., Bache, K.G., Raiborg, C., Trambaiolo, D., Wakatsuki, S., and Stenmark, H. (2005). Eap45 in mammalian ESCRT-II binds ubiquitin via a phosphoinositide-interacting GLUE domain. J. Biol. Chem. *280*, 19600–19606.
14. Saksena, S., Wahlman, J., Teis, D., Johnson, A.E., and Emr, S.D. (2009). Functional reconstitution of ESCRT-III assembly and disassembly. Cell *136*, 97–109.
15. Teis, D., Saksena, S., and Emr, S.D. (2008). Ordered assembly of the ESCRT-III complex on endosomes is required to sequester cargo during MVB formation. Dev. Cell *15*, 578–589.
16. Clague, M.J., Liu, H., and Urbé, S. (2012). Governance of endocytic trafficking and signaling by reversible ubiquitylation. Dev. Cell *23*, 457–467.
17. Agromayor, M., and Martin-Serrano, J. (2006). Interaction of AMSH with ESCRT-III and deubiquitination of endosomal cargo. J. Biol. Chem. *281*, 23083–23091.
18. Solomons, J., Sabin, C., Poudevigne, E., Usami, Y., Hulsik, D.L., Macheboeuf, P., Hartlieb, B., Göttlinger, H., and Weissenhorn, W. (2011). Structural basis for ESCRT-III CHMP3 recruitment of AMSH. Structure *19*, 1149–1159.
19. Row, P.E., Liu, H., Hayes, S., Welchman, R., Charalabous, P., Hofmann, K., Clague, M.J., Sanderson, C.M., and Urbé, S. (2007). The MIT domain of UBPY constitutes a CHMP binding and endosomal localization signal required for efficient epidermal growth factor receptor degradation. J. Biol. Chem. *282*, 30929–30937.
20. McCullough, J., Row, P.E., Lorenzo, O., Doherty, M., Beynon, R., Clague, M.J., and Urbé, S. (2006). Activation of the endosome-associated ubiquitin isopeptidase AMSH by STAM, a component of the multivesicular body-sorting machinery. Curr. Biol. *16*, 160–165.
21. Kato, M., Miyazawa, K., and Kitamura, N. (2000). A deubiquitinating enzyme UBPY interacts with the Src homology 3 domain of Hrs-binding protein via a novel binding motif PX(V/I)(D/N)RXXKP. J. Biol. Chem. *275*, 37481–37487.
22. Tanaka, N.N., Kaneko, K.K., Asao, H.H., Kasai, H.H., Endo, Y.Y., Fujita, T.T., Takeshita, T.T., and Sugamura, K.K. (1999). Possible involvement of a novel STAM-associated molecule "AMSH" in intracellular signal transduction mediated by cytokines. J. Biol. Chem. *274*, 19129–19135.
23. Row, P.E., Prior, I.A., McCullough, J., Clague, M.J., and Urbé, S. (2006). The ubiquitin isopeptidase UBPY regulates endosomal ubiquitin dynamics and is essential for receptor down-regulation. J. Biol. Chem. *281*, 12618–12624.
24. Bowers, K., Piper, S.C., Edeling, M.A., Gray, S.R., Owen, D.J., Lehner, P.J., and Luzio, J.P. (2006). Degradation of endocytosed epidermal growth factor and virally ubiquitinated major histocompatibility complex class I is independent of mammalian ESCRTII. J. Biol. Chem. *281*, 5094–5105.
25. Pareja, F., Ferraro, D.A., Rubin, C., Cohen-Dvashi, H., Zhang, F., Aulmann, S., Ben-Chetrit, N., Pines, G., Navon, R., Crosetto, N., et al. (2012). Deubiquitination of EGFR by Cezanne-1 contributes to cancer progression. Oncogene *31*, 4599–4608.

26. Alwan, H.A.J., and van Leeuwen, J.E.M. (2007). UBPY-mediated epidermal growth factor receptor (EGFR) de-ubiquitination promotes EGFR degradation. J. Biol. Chem. *282*, 1658–1669.
27. Mizuno, E., Kobayashi, K., Yamamoto, A., Kitamura, N., and Komada, M. (2006). A deubiquitinating enzyme UBPY regulates the level of protein ubiquitination on endosomes. Traffic *7*, 1017–1031.
28. Berlin, I., Schwartz, H., and Nash, P.D. (2010). Regulation of epidermal growth factor receptor ubiquitination and trafficking by the USP8·STAM complex. J. Biol. Chem. *285*, 34909–34921.
29. Mizuno, E., Iura, T., Mukai, A., Yoshimori, T., Kitamura, N., and Komada, M. (2005). Regulation of epidermal growth factor receptor down-regulation by UBPY-mediated deubiquitination at endosomes. Mol. Biol. Cell *16*, 5163–5174.
30. McCullough, J., Clague, M.J., and Urbé, S. (2004). AMSH is an endosome-associated ubiquitin isopeptidase. J. Cell Biol. *166*, 487–492.
31. Ma, Y.M., Boucrot, E., Villén, J., Affar, B., Gygi, S.P., Göttlinger, H.G., and Kirchhausen, T. (2007). Targeting of AMSH to endosomes is required for epidermal growth factor receptor degradation. J. Biol. Chem. *282*, 9805–9812.
32. Doyotte, A., Mironov, A., McKenzie, E., and Woodman, P. (2008). The Bro1-related protein HD-PTP/PTPN23 is required for endosomal cargo sorting and multivesicular body morphogenesis. Proc. Natl. Acad. Sci. USA *105*, 6308–6313.
33. Doyotte, A., Russell, M.R.G., Hopkins, C.R., and Woodman, P.G. (2005). Depletion of TSG101 forms a mammalian "Class E" compartment: a multicisternal early endosome with multiple sorting defects. J. Cell Sci. *118*, 3003–3017.
34. Richter, C., West, M., and Odorizzi, G. (2007). Dual mechanisms specify Doa4-mediated deubiquitination at multivesicular bodies. EMBO J. *26*, 2454–2464.
35. Razi, M., and Futter, C.E. (2006). Distinct roles for Tsg101 and Hrs in multivesicular body formation and inward vesiculation. Mol. Biol. Cell *17*, 3469–3483.
36. Ichioka, F., Takaya, E., Suzuki, H., Kajigaya, S., Buchman, V.L., Shibata, H., and Maki, M. (2007). HD-PTP and Alix share some membrane-traffic related proteins that interact with their Bro1 domains or proline-rich regions. Arch. Biochem. Biophys. *457*, 142–149.
37. Carlton, J.G., and Martin-Serrano, J. (2007). Parallels between cytokinesis and retroviral budding: a role for the ESCRT machinery. Science *316*, 1908–1912.
38. Fisher, R.D., Chung, H.Y., Zhai, Q., Robinson, H., Sundquist, W.I., and Hill, C.P. (2007). Structural and biochemical studies of ALIX/AIP1 and its role in retrovirus budding. Cell *128*, 841–852.
39. Harkiolaki, M., Tsirka, T., Lewitzky, M., Simister, P.C., Joshi, D., Bird, L.E., Jones, E.Y., O'Reilly, N., and Feller, S.M. (2009). Distinct binding modes of two epitopes in Gab2 that interact with the SH3C domain of Grb2. Structure *17*, 809–822.
40. Lohi, O., Poussu, A., Meriläinen, J., Kellokumpu, S., Wasenius, V.-M., and Lehto, V.-P. (1998). EAST, an epidermal growth factor receptor- and Eps15-associated protein with Src homology 3 and tyrosine-based activation motif domains. J. Biol. Chem. *273*, 21408–21415.
41. Umebayashi, K., Stenmark, H., and Yoshimori, T. (2008). Ubc4/5 and c-Cbl continue to ubiquitinate EGF receptor after internalization to facilitate polyubiquitination and degradation. Mol. Biol. Cell *19*, 3454–3462.
42. Kobayashi, H., Tanaka, N., Asao, H., Miura, S., Kyuuma, M., Semura, K., Ishii, N., and Sugamura, K. (2005). Hrs, a mammalian master molecule in vesicular transport and protein sorting, suppresses the degradation of ESCRT proteins signal transducing adaptor molecule 1 and 2. J. Biol. Chem. *280*, 10468–10477.
43. Söderberg, O., Gullberg, M., Jarvius, M., Ridderstråle, K., Leuchowius, K.-J., Jarvius, J., Wester, K., Hydbring, P., Bahram, F., Larsson, L.-G., and Landegren, U. (2006). Direct observation of individual endogenous protein complexes in situ by proximity ligation. Nat. Methods *3*, 995–1000.
44. Stern, K.A.K., Visser Smit, G.D., Place, T.L.T., Winistorfer, S.S., Piper, R.C.R., and Lill, N.L.N. (2007). Epidermal growth factor receptor fate is controlled by Hrs tyrosine phosphorylation sites that regulate Hrs degradation. Mol. Cell. Biol. *27*, 888–898.
45. Nikko, E., and André, B. (2007). Split-ubiquitin two-hybrid assay to analyze protein-protein interactions at the endosome: application to *Saccharomyces cerevisiae* Bro1 interacting with ESCRT complexes, the Doa4 ubiquitin hydrolase, and the Rsp5 ubiquitin ligase. Eukaryot. Cell *6*, 1266–1277.
46. Dores, M.R., Chen, B., Lin, H., Soh, U.J.K., Paing, M.M., Montagne, W.A., Meerloo, T., and Trejo, J. (2012). ALIX binds a YPX(3)L motif of the GPCR PAR1 and mediates ubiquitin-independent ESCRT-III/MVB sorting. J. Cell Biol. *197*, 407–419.
47. Matsuo, H., Chevallier, J., Mayran, N., Le Blanc, I., Ferguson, C., Fauré, J., Blanc, N.S., Matile, S., Dubochet, J., Sadoul, R., et al. (2004). Role of LBPA and Alix in multivesicular liposome formation and endosome organization. Science *303*, 531–534.
48. Sette, P., Mu, R., Dussupt, V., Jiang, J., Snyder, G., Smith, P., Xiao, T.S., and Bouamr, F. (2011). The Phe105 loop of Alix Bro1 domain plays a key role in HIV-1 release. Structure *19*, 1485–1495.
49. Shields, S.B.S., and Piper, R.C.R. (2011). How ubiquitin functions with ESCRTs. Traffic *12*, 1306–1317.
50. Eden, E.R., White, I.J., Tsapara, A., and Futter, C.E. (2010). Membrane contacts between endosomes and ER provide sites for PTP1B-epidermal growth factor receptor interaction. Nat. Cell Biol. *12*, 267–272.